Since January 2020 Elsevier has created a COVID-19 resource centre with free information in English and Mandarin on the novel coronavirus COVID-19. The COVID-19 resource centre is hosted on Elsevier Connect, the company's public news and information website.

Biosafety and Health xxx (2022) xxx–xxx

Contents lists available at ScienceDirect

Biosafety and Health

journal homepage: www.elsevier.com/locate/bsheal

Sequence difference of angiotensin-converting enzyme 2 between nonhuman primates affects its binding-affinity with SARS-CoV-2 S receptor binding domain

Xiaojun Zhou [a,1], Jingjing Zhao [b,1], Yefeng Qiu [c,*], Rui Jia [a,*]

[a] Department of Biosafety, China Biotechnology Co.LTD, Beijing 100025, China
[b] Department of Infectious Diseases, Beijing Chaoyang Hospital, Capital Medical University, Beijing 100043, China
[c] Laboratory Animal Center, Academy of Military Medical Sciences, Beijing 100071, China

ARTICLE INFO

Keywords:
SARS-CoV-2
Angiotensin-converting enzyme 2
Receptor binding domain
Surface plasmon resonance
African green monkey

ABSTRACT

Severe acute respiratory syndrome coronavirus 2 (SARS-CoV-2) has caused many deaths and contributed to a tremendous public health concern worldwide since 2020. Angiotensin-converting enzyme 2 (ACE2) binds to the SARS-CoV-2 virus as a receptor. The challenge of different nonhuman primate (NHP) species by SARS-CoV-2 virus demonstrated different effects on virus replication and disease pathology. This study characterizes differences between host ACE2 sequences of three NHP species: *Macaca mulatta, Macaca fascicularis,* and *Chlorocebus sabaeus*. In addition, the binding affinity between the ACE2 ectodomain and the SARS-CoV-2 S receptor-binding domain (RBD) was analyzed. Variation of ACE2 sequence among NHP species and the binding affinity may account for different susceptibility and responses to SARS-CoV-2 infection.

1. Introduction

Coronavirus disease 2019 (COVID-19), which was first reported in December 2019, resulted from severe acute respiratory syndrome coronavirus (SARS-CoV-2) infection [1]. Patients with COVID-19 presented with fever, pneumonia, and severe respiratory illness [2]. According to the World Health Organization, on June 13th, 2022, there were over 532 million confirmed cases globally, causing at least 6 million deaths. SARS-CoV-2 is a member of the betacoronavirus genus that closely resembles several bat coronaviruses and SARS-CoV [3,4]. Compared with SARS-CoV, SARS-CoV-2 seems to cause human-to-human transmission more quickly and has caused a pandemic for a long time on earth, leading to the WHO declaration of a Public Health Emergency of International Concern (PHEIC) [5,6].

The SARS-CoV spike protein (S) is cleaved into S1 and S2, mediating cell attachment and membrane fusion. ACE2, a cell-surface zinc peptidase, is the receptor of SARS-CoV or SARS-CoV-2 by binding to S1 receptor-binding domain (RBD) [7,8]. The S1 RBD fragment (residues 318 to 510) is sufficient for tight binding to the peptidase domain of ACE2 [9,10] and critical for virus-receptor interaction, which determines viral host range and tropism [11]. Changes in just a few residues in the SARS-CoV RBD can lead to efficient cross-species transmission [12,13]. The crystal structure of the ACE2 ectodomain, which binds the S1 RBD, demonstrates a claw-like *N*-terminal peptidase domain, with the active site at the base of a deep groove and a C-terminal "collectrin" domain [14]. ACE2 has been confirmed to be the receptor of SARS-CoV-2 recently [15], and a structural analysis also indicated that the SARS-CoV-2 S binds ACE2 with higher affinity than SARS-CoV S [16].

Animal models are essential for pathogenesis studies of viral infection, evaluation of antiviral treatments, and vaccine development. Several animal models of COVID-19 have been reported including hACE2-transgenic models [17,18], a non-transgenic mouse model [19], a golden hamster model [20], a ferret model [21], and NHP models [22,23]. Infection of SARS-CoV has been previously established in NHP, such as *Macaca mulatta* (referred to as rhesus macaca, RM), *Macaca fascicularis* (referred to as cynomolgus macaque, CM), and *Chlorocebus sabaeus* (referred to as African Green monkey, AGM), with varying levels of virus replication and serum neutralizing antibody production (*Chlorocebus sabaeus* > *Macaca fascicularis* > *Macaca mulatta*) [24]. The challenge of different NHP species, such as *Macaca mulatta, Macaca fascicularis,* and *Callithrix jacchus,* by SARS-CoV-2 virus infection also resulted in distinct effects in viral load and pathological changes [25]. However, the underlying factors are unclear.

* Corresponding authors.
E-mail addresses: qiuyefeng2001@163.com (Y. Qiu), jiarui@sinopharm.com (R. Jia).
[1] These authors contributed equally to this work.

https://doi.org/10.1016/j.bsheal.2022.09.001
Received 27 June 2022; Revised 5 September 2022; Accepted 5 September 2022
Available online xxxx

This study aims to characterize the NHP host ACE2 sequence and the binding affinity between the ACE2 ectodomain and SARS-CoV-2 S RBD.

2. Materials and methods

2.1. Data sources and commercial materials

The S protein sequence of SARS-CoV-2 comes from the complete genome of Wuhan seafood market pneumonia virus isolate Wuhan-Hu-1 with the NCBI reference sequence number NC_045512.2. The NCBI reference sequence numbers for ACE2 of different species are NM_001371415.1 for human, NM_001130513.1 for mouse, XM_005593037.3 for CM, NM_001135696 for RM, XM_007991113.1 for AGM. The SARS-CoV-2 S RBD was purchased from KMD Bioscience (Tianjin, China).

2.2. Cloning and sequencing of the ACE2 ectodomain of RM, CM, and AGM

Tissues of RM, CM, and AGM, were kindly provided by Dr. Yefeng Qiu of his laboratory animal Center. Total RNA was extracted from these tissues by the RNeasy Plus Universal Kit (Cat.No 73404, Qiagen) and reverse transcribed by the First Strand cDNA Synthesis Kit (Code No.FSK-101, Toyobo). The KOD-Plus- high fidelity PCR polymerase (Code No.KOD-201, Toyobo) was used to amplify the ACE2 genes of different species. Primers used for cloning the ACE2 ectodomain of AGM, RM, and CM are as follows: AGM-F: 5′-CTATATTGTTGTGATCC CATGG-3′, AGM-R: 5′-CATGTCACTTTCTGCAGCCA, RM-F: 5′-CATGT CAGGCTCTTCCTGGCTCC-3′, RM-R: 5′-CAACAGCAGCTTCATG GAATCCTTCAT-3′, CM-F: 5′-CATGTCAGGCTCTTCCTGGCTCC-3′, CM-R:5′-CCATCTCATGATGAGCTGT. The PCR conditions were 95℃ 5 min, 30 cycles of {92℃ 30 s, 55℃ 30 s, 72℃ 40 s}, 72℃ 5 min. The PCR products were purified by QIAquick Gel Extraction (Cat.No 28704, Qiagen) and sequenced by Sangon Biotech (Shanghai, China). The sequences obtained were aligned and compared with NM_001135696 for RM, XM_005593037.3 for CM, and XM_007991113.1 for AGM from the NCBI database. Moreover, the DNA sequences encoding the ACE2 ectodomain of humans, RM, AGM, CM, and mice were aligned by GeneDoc software.

2.3. Synthesizing and cloning of the ectoACE2-related genes of humans, CM, RM, and AGM

The 1101 bp genes which encode the ACE2 ectodomains of humans, CM, RM, and AGM, were synthesized by Sangon Biotech (Shanghai, China) and cloned into a pUC57 vector with the restriction enzyme site *Eco*RV at the 5′ end and a 6 × His tag as well as *Pac*I at 3′ end. After sequence confirmation, the DNA fragments with *Eco*RV and *Pac*I were cloned into the pCHO1.0 vector. Finally, the CHO1.0-ectoACE2 expression vectors were transformed into TOP10 competent cells and validated by restriction enzyme digestion and sequencing analysis.

2.4. Transfection, expression, and purification of the ACE2 ectodomains of different species

180 mL fresh Expi293™ Expression Medium (Cat.No A1435102, Thermo Scientific), which contains six mM L-glutamine, was used to resuspend 293F cells to a concentration of 1×10^6 cells/ml and be cultured at 37℃ in a shaking incubator with 5 % CO_2 the day before transfection. Moreover, 100 μg plasmid DNA was prepared by a Plasmid Plus Midi Kit (Cat. No 12945, Qiagen) and incubated with 200 μL Lipofectin™ (Cat. No 18292011, Thermo Scientific) within 20 mL Expi293™ Expression Medium at room temperature for 10 min. The transfected mixture was then added to 180 mL Expi293™ Expression Medium and cultured at 37℃ in a shaking incubator with 5 % CO_2. After being cultured for another four days, the transfected 293F cells and the cell culture supernatants were collected. Proteins extracted from the cells by M−PER Mammalian Protein Extraction Reagen (Cat.No 78503, Thermo Scientific) and the cell culture supernatants were purified using Ni Sepharose FF (Cat.No 17-5318-01, GE) and analyzed for expression of ACE2 by SDS-PAGE and western blot. A protease cocktail (Cat.No 5871, Cell Signaling) inhibited protein degradation. Protein Marker was purchased from Transgen Biotech (Cat. No DM211, China).

2.5. Surface plasmon resonance (SPR) analysis

His-tagged SARS-CoV-2 S RBD was diluted to 10 μg/ml by PBS and immobilized to an SA sensorchip (Cat. No 18–5019, Fortebio) using a Biacore X100 (GE Healthcare) and a running buffer composed of 10 mM HEPES pH 8.0, 150 mM NaCl and 0.05 % Tween 20. The ectoACE2 was diluted to a concentration of 200 nM by PBS buffer containing 0.1 % BSA and 0.02 % Tween20. The resulting data were fit to a 1:1 binding model using Fortebio Data Analysis 10.0 software (Fortebio).

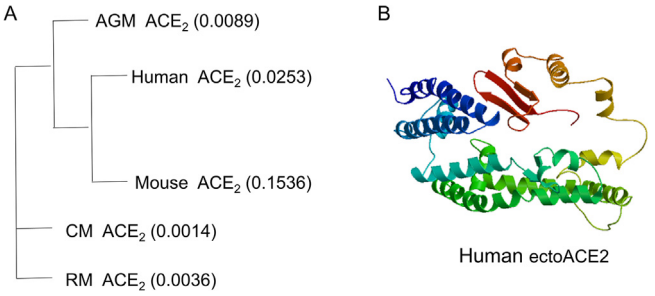

Fig. 1. Sequence variation and structure prediction of ACE2 among different species. A) Phylogenetic tree constructed based on sequence alignment of the full length (805aa) ACE2 amino acid sequences among human, mouse, RM, CM, and AGM. B) Predicted structure of the ectodomain of human ACE2.

Table 1
Contact residues of the SARS-CoV-2 RBD-ACE2 and SARS-CoV RBD-ACE2 interfaces.

SARS-CoV-2 RBD	ACE2	SARS-CoV RBD	ACE2
K417	Q24	R426	Q24
G446	T27	Y436	T27
Y449	F28	Y440	F28
Y453	D30	Y442	K31
L455	K31	L443	H34
F456	H34	L472	E37
A475	E35	N473	D38
F486	E37	Y475	Y41
N487	D38	N479	Q42
Y489	Y41	G482	L45
Q493	Q42	Y484	L79
G496	L79	T486	M82
Q498	M82	T487	Y83
T500	Y83	G488	Q325
N501	N330	I489	E329
G502	K353	Y491	N330
Y505	G354		K353
	D355		G354
	R357		D355
	R393		R357

2.6. Protein structure prediction

SWISS-MODEL performed automated protein structure homology modeling for ACE2 ectodomain via the ExPASy web server. The PDB file of the predicted protein was further analyzed through Swiss Pdb Viewer software.

3. Results

3.1. Sequence variations in ACE2 between different species

Sequence alignment of the total length (805aa) ACE2 amino acid sequences from the NCBI reference source of human, mouse, RM, CM, and AGM was performed, and a phylogenetic tree was constructed (Fig. 1). Residues in ACE2 that contact SARS-CoV-2 RBD and SARS-CoV RBD have been identified [8,26]. Therefore, the contact residues of the SARS-CoV-2 RBD-ACE2 and SARS-CoV RBD-ACE2 were listed in Table 1 [8].

Our results showed that position 101 residue of the AGM ectoACE2 DNA sequence was A while that of the NCBI sequence was C (Fig. 2A), resulting in a unique residue Pro^{34} of the AGM ectoACE2 amino acid sequence (Fig. 3). Position 574 G → A and 649 A → T transition of the RM ectoACE2 DNA sequence resulted in a change from Gly → Arg and Asn → Thr in amino acid sequence (Fig. 2B). No difference was found between the sequencing result of the CM ectoACE2 DNA and that of the NCBI sequence. A comparison of the ectoACE2 amino acid sequences between humans, RM, CM, and AGM found several different residues, as shown in Table 2. Compared with RM and humans, the residue Pro^{34} and residue Ala^{87} were unique in AGM. In

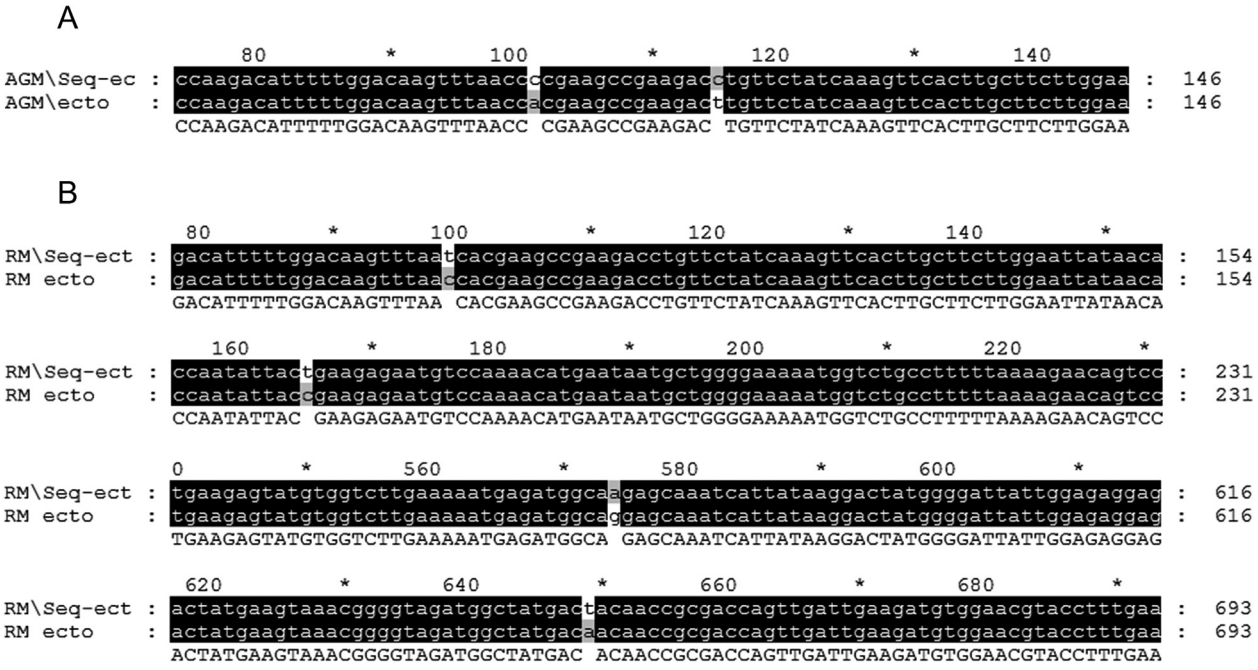

Fig. 2. Comparison of the obtained ACE2 ectodomain DNA sequence of RM, CM, and AGM with those of the NCBI database.

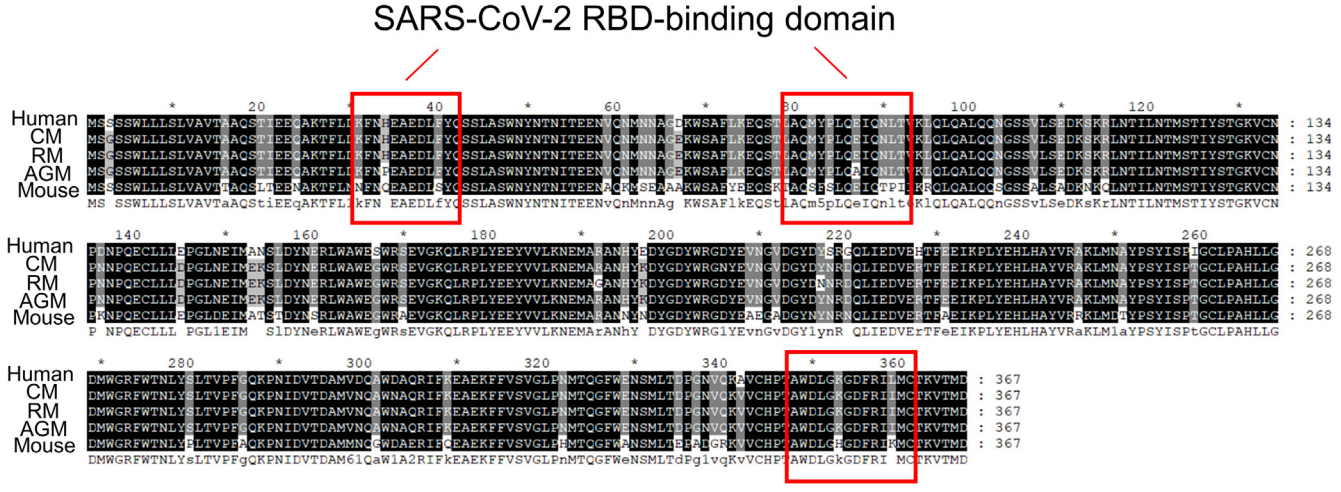

Fig. 3. Alignment of the *N*-terminal 367aa ectodomain of ACE2 among different species. The red box indicates three identified fragments in the ACE2 ectodomain critical for binding with SARS-CoV-2 or SARS-CoV RBD.

Table 2
Sequence identity of ACE2 *N*-terminal ectodomain in human, RM, CM, and AGM. Different residues in the *N*-terminal 367aa region ACE2 are listed by their position.

	3	34	67	87	136	145	153	154	167	193	217	218	220	228	259	299	303	342	359
Hu	S	H	D	E	D	E	A	N	S	R	Y	S	G	H	I	D	D	A	L
RM	G	H	E	E	N	D	E	K	G	G	N	N	D	R	T	N	N	V	I
AGM	G	P	E	A	N	D	E	K	G	R	Y	N	D	R	T	N	N	V	I
CM	G	H	E	E	N	D	E	K	G	R	Y	N	D	R	T	N	N	V	I

addition, the residues Asp67, Asp136, Asn154, Ser218, Gly220, His228, Ile259, Ala342, and Leu359, were unique in humans.

3.2. Modeling analysis of the ACE2 ectodomain structure within different species

The crystal structure of the ACE2 ectodomain shows a claw-like *N*-terminal peptidase domain, with the active site at the base of a deep groove and a C-terminal "collectrin" domain [13]. Prediction of the ACE2 ectodomain demonstrated a similar "pocket" structure (Fig. 1B). The previous study has identified three fragments (31 ~ 41aa, 82 ~ 93aa, 353 ~ 357aa) in ACE2 ectodomain which are critical for binding with SARS-CoV RBD as well as SARS-CoV-2 RBD [10,26], among which residue Pro34 and residue Ala87 in AGM were different from His34 and Glu87 in human and RM (Table 2). We found that these three fragments are part of a prominent "gap" structure through structure modeling. The other two "gap" structures are formed at residues 217, 218, 220, 228, and 299 and 303, respectively. The glycosylation sites, residue 218, 299, 303 of RM and AGM ACE2 all contain Asn that appears to influence interaction with SARS-CoV S RBD by introducing a glycan.

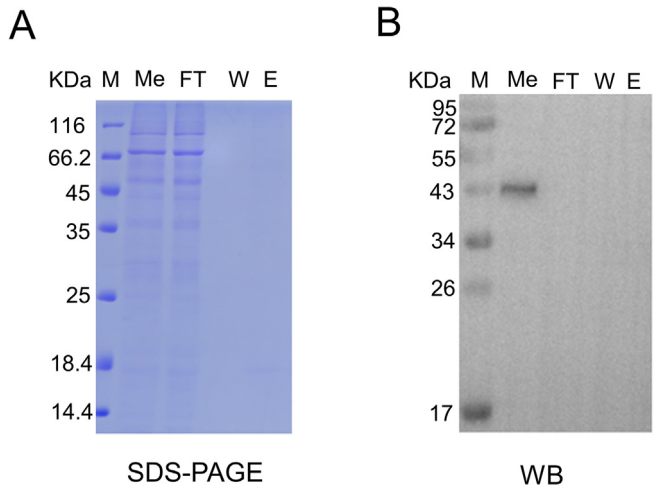

Fig. 4. Expression analysis of the RM ACE2 ectodomain protein. M, Me, FT, W, E stands for the protein marker, culture medium, the flow through fraction, the washing fraction, eluted fraction, respectively.

3.3. Expression of the ecto-ACE2 proteins and SPR analysis

SDS-PAGE and western blot analysis have confirmed the expression of the ectoACE2 protein in the cultured 293F cells instead of the supernatants (Fig. 4). In contrast, SPR analysis demonstrated the binding characteristics between SARS-CoV-2 S RBD and ectoACE2 (Fig. 5). The dissociation constant (K_D) between SARS-CoV-2 S RBD and ectoACE2 from human, RM, CM, and AGM were 61.2 nM, 68.0 nM, 69.2 nM, 67.6 nM (Fig. 5), respectively, indicating a decreased binding affinity (Human > AGM > RM > CM).

4. Discussion

ACE2 is a membrane protein located in the lung, heart, kidney, and intestine [27,28] with a physiological role in facilitating the maturation of angiotensin, which controls vasoconstriction and blood pres-

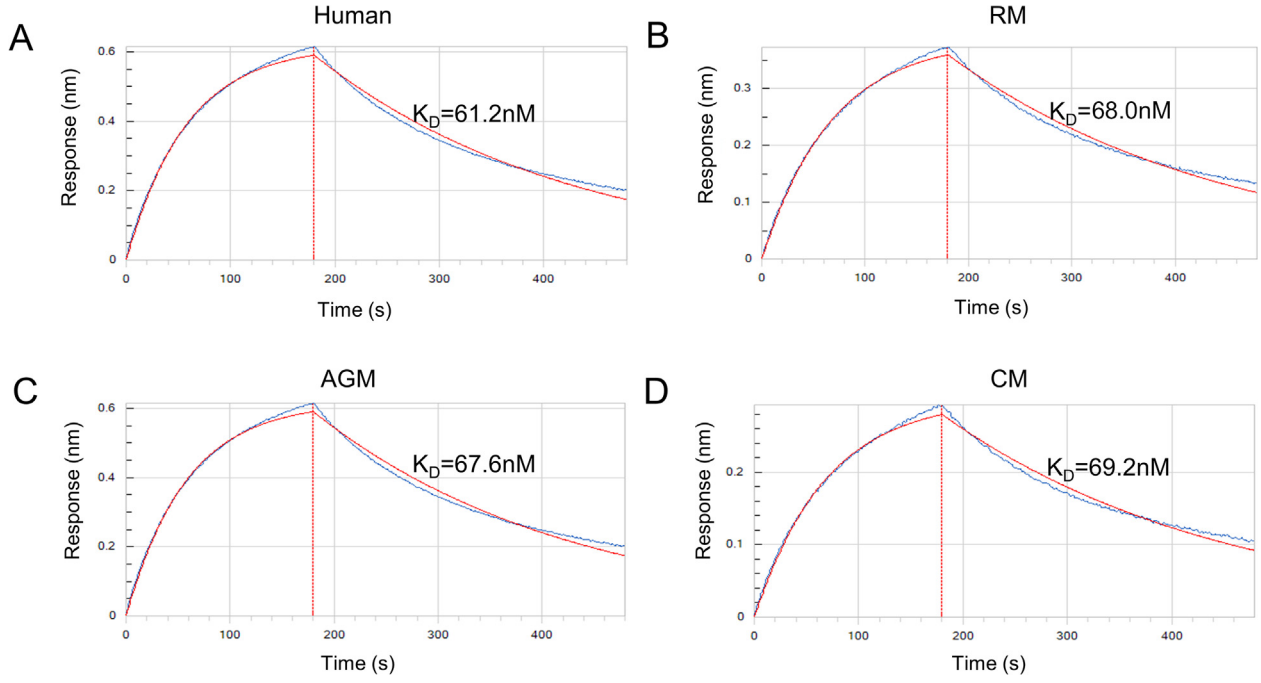

Fig. 5. SPR determination of the affinity between SARS-CoV-2 S RBD and ACE2 *N*-terminal ectodomain of different species. K_D indicates dissociation constant.

sure. As the receptors of both SARS-CoV and SARS-CoV-2, ACE2 has drawn attention for its potential use in drug or vaccine design. However, the results also need elaboration of the structure and interaction between ACE2 and S RBD from SARS-CoV or SARS-CoV-2. A recent study has revealed the 2.9 Å resolution cryo-EM structure of full-length human ACE2 in complex with B^0AT1 (SLC6A19)[29], which interacts with ACE2 for the neutral amino acid transport on the surface of intestinal cells [30]. This study demonstrated open and closed conformations of the ACE2-B^0AT1 complex and a newly resolved Collectrin-like domain (CLD) on ACE2, which mediates homodimerization. Also, it was found that expression of ACE2 from baculovirus-infected insect cells or mammalian cells results in different glycosylation sites on the surface of ACE2 peptidase domains. Furthermore, a previous study has shown that chloroquine inhibits SARS-CoV infection by interfering with the terminal glycosylation of ACE2 [31], indicating the significance of glycosylation in recognizing viruses and receptors.

Several species can be infected by SARS-CoV-2, such as bats, golden hamsters, ferrets, and even horses, indicating a highly transmissible capacity across different species by SARS-CoV-2. As for NHPs, our data demonstrated differences in several residues of the ACE2 ectodomain between humans, RM, CM, and AGM. The AGM-specific Pro34 and residue Ala87 are located in the 31 ~ 41aa and 82 ~ 93aa fragments of ACE2 ectodomain, respectively. The specific residues Asn217, Asn218, Asp220, and Arg228 form a slightly different “gap” structure. Also, variations at the glycosylation sites 136, 154, 217, 218, 299, and 303 among humans, RM, and AGM may result in different binding affinity between ACE2 ectodomain and SARS-CoV-2. Compared with the Old World monkey *Macaca fascicularis* and the New World monkey *Callithrix jacchus*, *Macaca mulatta* showed the most robust responses to SARS-CoV-2 infection, including increased inflammatory cytokine expression and pathological changes in the pulmonary tissues [25]. A recent study performed a challenge of SARS-CoV-2 by aerosol in *Macaca mulatta* (rhesus macaque) and *Chlorocebus aethiops* (African green monkey) [32]. Moreover, the results indicated that aerosol particle production increase relative to pre-infection totals was more profound in the rhesus macaques than in the African green monkeys. Compared with the African green monkey, our data demonstrated a slightly higher binding affinity between the ACE2 ectodomain of rhesus macaque and SARS-CoV-2. Variation of ACE2 sequence among NHP species and the binding affinity may account for different susceptibility and responses to SARS-CoV-2 infection, which may provide insights into the virus-host interaction, drugs, or vaccine design.

Declaration of Competing Interest

The authors declare that there are no conflicts of interest.

Author contributions

Xiaojun Zhou: Conceptualization, Methodology, Writing – original draft. **Jingjing Zhao:** Investigation, Resources. **Yefeng Qiu:** Supervision, Resources. **Rui Jia:** Writing – review & editing.

References

[1] J.F.W. Chan, S. Yuan, K.H. Kok, K.K. To, H. Chu, J. Yang, F. Xing, J. Liu, C.C. Yip, R.W. Poon, et al, A familial cluster of pneumonia associated with the 2019 novel coronavirus indicating person-to-person transmission: a study of a family cluster, Lancet 395 (10223) (2020) 514–523, https://doi.org/10.1016/S0140-6736(20)30154-9.

[2] C. Huang, Y. Wang, X. Li, L. Ren, J. Zhao, Y. Hu, L. Zhang, G. Fan, J. Xu, X. Gu, et al, Clinical features of patients infected with 2019 novel coronavirus in Wuhan, China, Lancet 395 (10223) (2020) 497–506, https://doi.org/10.1016/S0140-6736(20)30183-5.

[3] R. Lu, X. Zhao, J. Li, P. Niu, B. Yang, H. Wu, W. Wang, H. Song, B. Huang, N. Zhu, et al, Genomic characterisation and epidemiology of 2019 novel coronavirus: implications for virus origins and receptor binding, Lancet 395 (10224) (2020) 565–574, https://doi.org/10.1016/S0140-6736(20)30251-8.

[4] F. Wu, S. Zhao, B. Yu, Y.M. Chen, W. Wang, Z. Song, Y. Hu, Z. Tao, J. Tian, Y. Pei, et al, A new coronavirus associated with human respiratory disease in China, Nature 579 (7798) (2020) 265–269, https://doi.org/10.1038/s41586-020-2008-3.

[5] N. Chen, M. Zhou, X. Dong, J. Qu, F. Gong, Y. Han, Y. Qiu, J. Wang, Y. Liu, Y. Wei, et al, Epidemiological and clinical characteristics of 99 cases of 2019 novel coronavirus pneumonia in Wuhan, China: a descriptive study, Lancet 395 (10223) (2020) 507–513, https://doi.org/10.2139/ssrn.3523861.

[6] Q. Li, X. Guan, P. Wu, X. Wang, L. Zhou, Y. Tong, R. Ren, K. Leung, E. Lau, J.Y. Wong, et al, Early transmission dynamics in Wuhan, China, of novel coronavirus-infected pneumonia, N. Engl. J. Med. 382 (13) (2020) 1199–1207, https://doi.org/10.1056/NEJMoa2001316.

[7] W. Li, M.J. Moore, N. Vasilieva, J. Sui, S.K. Wong, M.A. Berne, M. Somasundaran, J.L. Sullivan, K. Luzuriaga, T.C. Greenough, et al, Angiotensin-converting enzyme 2 is a functional receptor for the SARS coronavirus, Nature 426 (6965) (2003) 450–454, https://doi.org/10.1038/nature02145.

[8] J. Lan, J.W. Ge, J.F. Yu, S.S. Shan, H. Zhou, S.L. Fan, Q. Zhang, X.L. Shi, Q.S. Wang, L.Q. Zhang, et al, Structure of the SARS-CoV-2 spike receptor-binding domain bound to the ACE2 receptor, Nature 581 (7807) (2020) 215–220, https://doi.org/10.1038/s41586-020-2180-5.

[9] S.K. Wong, W. Li, M.J. Moore, H. Choe, M. Farzan, A 193-amino acid fragment of the SARS coronavirus S protein efficiently binds angiotensin-converting enzyme 2, J. Biol. Chem. 279 (5) (2004) 3197–3201, https://doi.org/10.1074/JBC.C300520200.

[10] G.J. Babcock, D.J. Esshaki, W.D. Thomas, D.M. Ambrosino, Amino acids 270 to 510 of the severe acute respiratory syndrome coronavirus spike protein are required for interaction with receptor, J. Virol. 78 (9) (2004) 4552–4560, https://doi.org/10.1128/jvi.78.9.4552-4560.2004.

[11] W. Li, C. Zhang, J. Sui, J.H. Kuhn, M.J. Moore, S. Luo, S.K. Wong, I.C. Huang, K. Xu, N. Vasilieva, et al, Receptor and viral determinants of SARS-coroavirus adaptation to human ACE2, EMBO. J. 24 (8) (2005) 1634–1643, https://doi.org/10.1038/sj.emboj.7600640.

[12] Y. Guan, B.J. Zheng, Y.Q. He, X.L. Liu, Z.X. Zhuang, C.L. Cheung, S.W. Luo, P.H. Li, L.J. Zhang, Y.J. Guan, et al, Isolation and characterizationof viruses related to the SARS coronavirus from animals in southern China, Science 302 (5643) (2003) 276–278, https://doi.org/10.1126/science.1087139.

[13] H.D. Song, C.C. Tu, G.W. Zhang, S.Y. Wang, K. Zheng, L.C. Lei, Q.X. Chen, Y.W. Gao, H.Q. Zhou, H. Xiang, et al, Cross-host evolution of severe acute respiratory syndrome coronavirus in palm civet and human, Proc. Natl. Acad. Sci. U. S. A. 102 (7) (2005) 2430–2435, https://doi.org/10.1073/pnas.0409608102.

[14] P. Towler, B. Staker, S.G. Prasad, S. Menon, J. Tang, T. Parsons, D. Ryan, M. Fisher, D. Williams, N.A. Dales, et al, ACE2 X-ray structures reveal a large hinge-bending motion important for inhibitor binding and catalysis, J. Biol. Chem. 279 (17) (2004) 17996–18007, https://doi.org/10.1074/jbc.M311191200.

[15] P. Zhou, X. Yang, X. Wang, B. Hu, L. Zhang, W. Zhang, H. Si, Y. Zhu, B. Li, C. Huang, et al, Discovery of a novel coronavirus associated with the recent pneumonia outbreak in humans and its potential bat origin, Nature 579 (2020) 270–273, https://doi.org/10.1101/2020.01.22.914952.

[16] D. Wrapp, N. Wang, K.S. Corbett, J.A. Goldsmith, C.L. Hsieh, O. Abiona, B.S. Graham, J.S. McLellan, Cryo-EM Structure of the 2019-nCoV Spike in the Prefusion Conformation, Science 367 (6483) (2020) 1260–1263, https://doi.org/10.1101/2020.02.11.944462.

[17] S.H. Sun, Q. Chen, H.J. Gu, G. Yang, Y.X. Wang, X.Y. Huang, S.S. Liu, N.N. Zhang, X.F. Li, R. Xiong, et al, A mouse models of SARS-CoV-2 Infection and Pathogenesis, Cell. Host & Microbe. 28 (1) (2020) 124–133, https://doi.org/10.1016/j.chom.2020.05.020.

[18] L.L. Bao, W. Deng, B.Y. Huang, H. Gao, J.N. Liu, L.L. Ren, Q. Wei, P. Yu, Y.F. Xu, F. F. Qi, et al, The pathogenicity of SARS-CoV-2 in hACE2 transgenic mice, Nature 583 (7818) (2020) 830–833, https://doi.org/10.1038/s41586-020-2312-y.

[19] A.O. Hassan, J.B. Case, E.S. Winkler, L.B. Thackray, N.M. Kafai, A.L. Bailey, B.T. McCune, J.M. Fox, R.E. Chen, W.B. Alsoussi, et al, A SARS-CoV-2 infection model in mice demonstrate protection by neutralizing antibodies, Cell 182 (3) (2020) 744–753, https://doi.org/10.1016/j.cell.2020.06.011.

[20] J.F.W. Chan, A.J.X. Zhang, S.F. Yuan, V.K.M. Poon, C.C.S. Chan, A.C.Y. Lee, W. M. Chan, Z.M. Fan, H.W. Tsoi, L. Wen, et al, Simulation of the clinical and pathological manifestation of coronavirus disease 2019 (COVID-19) in golden Syrian hamster model: implications for disease pathogenesis and transmissibility, Clin. Infect. Dis. 71 (9) (2020) 2428–2446, https://doi.org/10.1093/cid/ciaa325.

[21] Y. Kim, S.G. Kim, S.M. Kim, E.H. Kim, S.J. Park, K.M. Yu, J.H. Chang, E.J. Kim, S.H. Lee, M.A.B. Casel, et al, Infection and rapid transmission of SARS-CoV-2 in ferrets, Cell. Host & microbe. 27 (5) (2020) 704–709, https://doi.org/10.1016/j.chom.2020.03.023.

[22] P. Yu, F.F. Qi, Y.F. Xu, F.D. Li, P.P. Liu, J.Y. Liu, L.L. Bao, W. Deng, H. Gao, Z.G. Xiang, et al, Age-related rhesus macaque models of COVID-19, Animal. Model. Exp. Med. 3 (1) (2020) 93–97, https://doi.org/10.1002/ame2.12108.

[23] C. Shan, Y.F. Yao, X.L. Yang, Y.W. Zhou, G. Gao, Y. Peng, L. Yang, X. Hu, J. Xiong, R.D. Jiang, et al, Infection with novel coronavirus (SARS-CoV-2) causes pneumonia in Rhesus macaques, Cell. research. 30 (8) (2020) 670–677, https://doi.org/10.1038/s41422-020-0364-z.

[24] J. McAuliffe, L. Vogel, A. Roberts, G. Fahle, S. Fischer, W.J. Shieh, E. Butler, S. Zaki, M. St. Claire, B. Murphy, et al, Replication of SARS coronavirus administered into the respiratory tract of African Green, rhesus and cynomolgus monkeys, Virol 330 (1) (2004) 8–15, https://doi.org/10.1016/j.virol.2004.09.030.

[25] S.Y. Lu, Y. Zhao, W.H. Yu, Y. Yang, J.H. Gao, J.B. Wang, D.X. Kuang, J. Yang, C.X. Ma, J.W. Xu, et al, Comparison of nonhuman primates identified the suitable model for COVID-19, Signal. Transduct. Tar. 5 (1) (2020) 157, https://doi.org/10.1038/s41392-020-00269-6.

[26] F. Li, W. Li, M. Farzan, S.C. Harrison, Structure of SARS coronavirus spike receptor-binding domain complexed with receptor, Science. 309 (5742) (2005) 1864–1868, https://doi.org/10.1126/science.1116480.

[27] M. Donoghue, F. Hsieh, E. Baronas, K. Godbout, M. Gosselin, N. Stagliano, M. Donovan, B. Woolf, K. Robison, R. Jeyaseelan, et al, A novel angiotensin-converting enzyme -related carboxypeptidase (ACE2) converts angiotensin I to angiotensin 1–9, Circ Res. 87 (5) (2000) E1–E9, https://doi.org/10.1161/01.res.87.5.e1.

[28] H. Zhang, Z. Kang, H. Gong, D. Xu, J. Wang, Z. Li, X. Cui, J. Xiao, T. Meng, W. Zhou, et al, The digestive system is a pontential route of 2019-nCoV infection: a bioinformatics analysis based on single-cell transcriptomes [Preprint], bioRxiv. (2020), https://doi.org/10.1101/2020.01.30.927806.

[29] R. Yan, Y. Zhang, Y. Li, L. Xia, Q. Zhou, Structure of dimeric full-length human ACE2 in complex with B0AT1, Science 367 (6485) (2020) 1444–1448, https://doi.org/10.1101/2020.02.17.951848.

[30] H.F. Seow, S. Broer, A. Broer, C.G. Bailey, S.J. Potter, J.A. Cavanaugh, J.E. Rasko, Hartnup disorder is caused by mutation in the gene encoding the neutral amino acid transporter SLC6A19, Nat. Genet. 36 (9) (2004) 1003–1007, https://doi.org/10.1038/ng1406.

[31] M.J. Vincent, E. Bergeron, S. Benjannet, B.R. Erickson, P.E. Rollin, T.G. Ksiazek, N. G. Seidah, S.T. Nichol, Chloroquine is a potent inhibitor of SARS coronavirus infection and spread, Virol. J. 2 (2005) 69, https://doi.org/10.1186/1743-422X-2-69.

[32] D.A. Edwards, D. Ausiello, J. Salzman, T. Devlin, R. Langer, B.J. Beddingfield, A.C. Fears, L.A. Doyle-Meyers, R.K. Redmann, S.Z. Killeen, et al, Exhaled aerosol increases with COVID-19 infection, age, and obesity, Proc. Natl. Acad. Sci. U. S. A. 118 (8) (2021) e2021830118, https://doi.org/10.1073/pnas.2021830118.